Using Satellite-Observed uv Intensities to Deduce Electron Density Profiles

D.J. Strickland* and R.E. Daniell†
Beers Associates, Inc., Reston, Virginia

and

J.R. Jasperse‡
Air Force Geophysics Laboratory, Bedford, Massachusetts

This paper addresses the problem of monitoring daytime and auroral ionospheres using optical measurements from satellites. The most attractive approach is to use optical emission features of the neutral atmosphere to monitor both source variability and neutral density and composition. From this information, the electron density profile may be deduced subject to uncertainties caused by neutral winds and electric fields. Emission features, which we examine as candidates for use in this approach, are bands of the N_2 LBH system, N_2 Vegard-Kaplan 2762 Å, N_2^+ 1N 3914 Å, and the atomic oxygen lines at 1356 and 2972 Å. Calculated intensities of these features and n_e are shown for daytime and auroral conditions.

Introduction

IN this paper, we shall discuss work in progress, the goal of which is to assess the utility of satellite-observed optical emission features in deducing the E and F region electron density distributions (n_e). Here we restrict ourselves to the daytime E and F regions and to the auroral E region. We know of no emission feature in these regions that gives a direct signature of the ions present, unlike, say, the O^+ recombination emissions in the tropical nighttime airglow.[1,2] O^+ 834 Å comes closest to fulfilling the requirement since O^+ can affect the 834 Å intensity through multiple scattering.[3] This in itself poses a difficult problem which we shall not address here. It then becomes a two-step process to obtain n_e from optical measurements. We must first obtain a representation of the source (solar ionizing spectrum or incident auroral electron spectrum), followed by its use in calculating n_e. The emphasis in this paper will be on how well the source spectrum can be determined from optical data. To address the second step, we give examples of the sensitivity of n_e to variations in the source spectrum.

The variability of n_e can pose some serious problems for the above technique. This variability is caused by 1) time and spatial changes in the source, 2) the same type of changes in the major neutral density profiles, and 3) mechanics which produce bulk transport of the plasma. As noted above, item 1 shall receive most of our attention. Item 2 is important because uncertainties introduced can affect both the accuracy of the deduced source spectrum and the subsequently calculated n_e profile. The accuracy of n_e is dependent not only on the assumed source spectrum, but also on assumed neutral densities through chemistry and diffusion. More shall be said about item 2 in the third section. Item 3 has to do with winds and fields and will be briefly discussed in the next section. Beyond this, however, we shall restrict ourselves to conditions for which n_e is dependent only on the ionizing source.

We shall examine N_2 LBH 1383 Å and OI 1356 Å in the dayglow. For auroral conditions, we shall consider these as well as OI 2972 Å; the LBH bands at 1273, 1325, and 1354 Å; N_2 Vegard-Kaplan (VK) 2762 Å; and N_2^+ 1N 3914 Å. Some of the auroral results to follow have recently been discussed in more detail in the paper by Strickland et al.[4] In particular, these authors determined the variability of nadir viewing satellite-observed intensities for OI 1356, N_2^+ 3914 Å, and LBH bands at 1273, 1325, and 1383 Å as a function of electron spectral hardness and model atmosphere. The causes of variability in the relative intensities among the above features are variations in 1) excitation efficiencies, 2) pure photon absorption (here due to O_2), and 3) chemical processes (quenching, in particular) that are due to changes in source and neutral atmospheric conditions. Results will follow that demonstrate the strengths of these effects on the emissions.

Ionospheric Variability Due to Neutral Winds and Electric Fields

In the F region ionosphere (above 180 km) both the ion-neutral and electron-neutral collision frequencies are much less than the respective gyrofrequencies. This means that the mobility of a charged particle is much greater along a field line than across field lines. The neutral winds of the thermospheric circulation produce a frictional force on the ionospheric plasma, but only the component of that force which acts along a field line is effective at imparting motion to the plasma. Magnetic field lines lie approximately in meridional planes and rise in altitude toward the equator. During daytime hours, the normal thermospheric circulation is from equator to pole,[5,6] which tends to drive the plasma downward. This reduces not only the altitude of the ionization peak, but also the peak concentration, since chemical losses are larger at lower altitudes. At middle latitudes the effects of these winds can be as important as diffusion, resulting in a lowering of the F_2 peak by ~ 50 km and a reduction in peak electron density by ~ 35%.[7,8] However, the thermospheric circulation is quite variable on a daily basis, which makes the ionospheric variability difficult to predict. One source of variability is the energy deposited at high latitudes during geomagnetic substorms which can alter the global thermospheric circulation and even reverse the direction of flow.[6,9] Furthermore, the resistance of ions to cross-field motion can alter the thermospheric winds in the altitude regime above 300 km, further complicating the picture.

In the E region ionosphere (150-160 km) the ion cross-field mobility is considerably larger than that of electrons. In this

Received Jan. 24, 1983; revision submitted Aug. 29, 1983.

*Senior Scientist.

†Scientist.

‡Scientist, Ionospheric Dynamics Branch, Space Physics Division.

altitude regime, neutral winds induce a charge separation which results in a global electric field system. Because magnetic field lines are nearly equipotentials, this electric field system is mapped into the F region, where it causes plasma ($E \times B$) drifts.[7] One may think of the E region winds acting as a dynamo generator while the F region plasma responds as an electric motor. The effect of the electric field is generally smaller than that due to F region winds and varies throughout the day.

In addition to the large-scale effects caused by thermospheric winds and the dynamo electric field, there are small-scale structures—ionospheric irregularities—which have a variety of sources.[7] The irregularities are present in both the E and F regions and at all latitudes.[10,11] At auroral and equatorial latitudes the primary causes of ionospheric irregularities are plasma instabilities, although the relative importance of neutral dynamics in the explanation of equatorial spread F is subject to debate. At midlatitudes, the situation is less well understood. Wind shears are known to produce sporadic E layers while traveling ionospheric disturbances have been explained by gravity waves propagating from below or from the auroral zone. A number of plasma mechanisms have been proposed to explain smaller-scale structures, but verification of these hypotheses awaits more complete sets of observational data.[11]

Both E and F region thermospheric winds can have a significant influence on the electron distribution above 200 km or so. They are hard to observe and continue to be the subject of theoretical and experimental research. If the winds are known, their effects on the ionosphere can be determined.[4] The principal implication for satellite monitoring of the ionosphere is that some method of measuring or calculating thermospheric winds must be developed. Global models of the thermospheric circulation provide a useful beginning, but the effects of geomagnetic activity must also be included if reasonable accuracy is to be obtained. Since ionospheric irregularities are less well understood, particularly at midlatitudes, they present a formidable problem for satellite monitoring. Those problems are not addressed further in this paper, but remain important research subjects.

Emission Variability due to Sources and Neutral Atmosphere

The technique being addressed is most attractive for situations in which the density profiles of N_2, O_2, and O are known. Under those conditions, variability of one optical intensity relative to another with changes in either time or location can be directly related to variability in source conditions. However, the neutral density profiles cannot be precisely known because of their intrinsic variability and the difficulty of precisely describing that variability. The latter problem is due to the approximate nature of existing thermospheric density models (for recent models, see Refs. 12-16) and to the limitations of measurement techniques. Of particular interest here are satellite-based measurements. In situ measurements can be expected to be the most reliable, but may be insufficient for specifying altitude profiles to the degree of accuracy desired. Optical remote sensing techniques, on the other hand, do hold a potential for measuring column densities, which can be used to scale corresponding volume density profiles. This problem is addressed next. One of the objectives of the present work must be to determine just how precisely the major neutral densities need to be known to make the technique under investigation practical. The required precision is dependent on source conditions and, of course, on instrumental conditions.

The problem raised above is whether it is possible to separate the effects of neutral density variations from source variations when using optical data. Various researchers are actively investigating the problem of sensing the neutral atmosphere.[17-19] Their concern has been with the analysis of satellite-observed limb profiles for features such as OI 1356 Å and N_2 LBH bands. We have concentrated our efforts on nadir viewing observations, and we believe that, with the right choice of features and instrumental parameters, the source and atmospheric variabilities can be decoupled. This is strengthened by the fact that there are limitations to the relative variability between the N_2 and O_2 densities in the regions of peak excitation (for either auroral or daytime conditions). Furthermore, the models cited above are probably more than adequate under most observing conditions for describing these relative densities. It then becomes attractive to use selected N_2 band emissions for initially characterizing the source spectrum. For auroral conditions, their relative strengths indicate the hardness of the electron source spectrum through either of the basic mechanisms of pure absorption or quenching, depending on the features. Given a representation of the spectral hardness, the magnitudes of the observed intensities then determine the energy content of the spectrum. In the daytime ionosphere, most of the F region ionization is produced by radiation in the range 100-800 Å with a smaller contribution from the 800-910 Å range.[8] The radiation below 150 Å produces only 5 to 8% of the ionization, depending on solar activity. Since the shape of the solar spectrum in the wavelength range 150-910 Å does not vary drastically with solar activity,[8] the important parameter is the energy content of that part of the spectrum. The magnitudes of the observed airglow intensities provide a measure of that parameter. However, the variability of the ultraviolet dayglow is not well understood. Rocket data analyzed by Meier et al. (Ref. 20 and personal communication) indicate that the variability is weaker than the results presented below would suggest. This remains an area of active investigation.

With an initial characterization of the source spectrum, we may turn to the problem of better determining the neutral densities. The atomic oxygen density is of prime interest, since it probably experiences the greatest relative variation (see above papers on thermospheric modeling) and has associated with it some key uv emission features (examples are OI 1304 Å, OI 1356 Å, and OI 2972 Å). Because O is a minor species when considered over the entire excitation region, its optical intensities are sensitive to its overall density. Thus, given the source spectrum, a measure of, say, the OI 1356 Å intensity (with a minor contamination from N_2 LBH 1354 Å) gives a direct measure of the magnitude of the O density profile. We may now repeat the process to further improve both the source representation and neutral density description.

Computational Models

Daytime Ionosphere

We possess two models and associated computer codes for describing the interactions of solar ionizing radiation and photoelectrons with the atmosphere. One is the Boltzmann-Fokker-Planck model of Jasperse,[21,22] which provides detailed energy spectra of the electrons over both the thermal and photoelectron energy regions. The other model is by Strickland and Meier,[23] and also gives photoelectron spectra, but with a less detailed description of the Boltzmann collision integral. In the second model, more emphasis is placed on the calculation of optical intensities. Chemistry codes are coupled to the abovementioned photoelectron codes to calculate temperatures, ion densities, and various neutral densities. Results to follow will come from the use of the second photoelectron model mentioned above and associated chemistry code which allows for O^+ diffusion.

Auroral Ionosphere

The electron transport model of Strickland et al.[24] is used to specify the electron spectrum and associated excitation and ionization rates. A Boltzmann equation is solved which gives the spectrum or distribution function from the highest primary energy of interest down to the eV range. Electron interactions

are limited to the particle-particle type, which includes elastic scattering, excitation, and ionization leading to energy loss of the incident electron and production of a secondary electron. A time-dependent chemistry code is coupled to the transport results and gives the densities of numerous ions and neutrals, along with intensities for a variety of emission features. This code is essentially the same as the one from which the daytime results to follow were obtained.

Comparisons with Optical, Electron, and Ion Data

The calculation of photoelectron and auroral electron spectra, excitation rates, chemical species, densities, and optical intensities involves a large body of input data and the use of some large computer codes. It is essential to compare these calculated quantities with independent results as well as measurements prior to a serious investigation of the problem being addressed. Three such comparisons follow.

We first note that electron spectra are the most difficult to calculate the abovementioned quantities. We have tested them through various comparisons and by observing how well they conserve energy. The latter test typically yields an error of less than 10%. The auroral electron results have been well tested, beginning with comparisons discussed by Strickland et al.[4] followed by subsequent comparisons with rocket and satellite data. This latter work is unpublished but does generally show good agreement. Specific examples of applied data are the rocket data of Spiger and Anderson[25] and satellite data of Craven and Frank.[26] The observed quantity is the auroral electron spectrum given as a function of both energy and angle. With regard to the calculated photoelectron spectra, excellent agreement has been achieved with both data and independent calculations. These comparisons may be seen in the report of Strickland and Meier.[23]

For the comparisons to follow, we have chosen optical, ion density, and electron density data, since these are the types of data we are ultimately interested in. We begin with the electron density information in Fig. 1, which comes from Jasperse.[22] This figure shows good overall agreement between theory and experiment for daytime conditions. An example of fractional ion abundances under auroral conditions is shown in Fig. 2. The data come from Swider and Narcisi[28] and were obtained with an ion mass spectrometer mounted on a rocket fired into the continuous aurora. The calculated results show good overall agreement, with the exception of those for N_2^+ which lie above the data. For this same experiment, satisfactory agreement was also obtained between the calculated electron density and coincident radar data. As an example of a comparison with optical data, we show in Fig. 3 results from Strickland and Anderson[29] which give the 1356 Å limb intensity for daytime conditions. The data were provided by Newman and Christensen from a spectrometer experiment on board satellite DMSP-F4.[17,19] Calculations of the needed photoelectron spectra and excitation rates come from the second of the previously discussed photoelectron models,[23] while the remaining calculations were provided by the photon transport model of Anderson et al.[30]

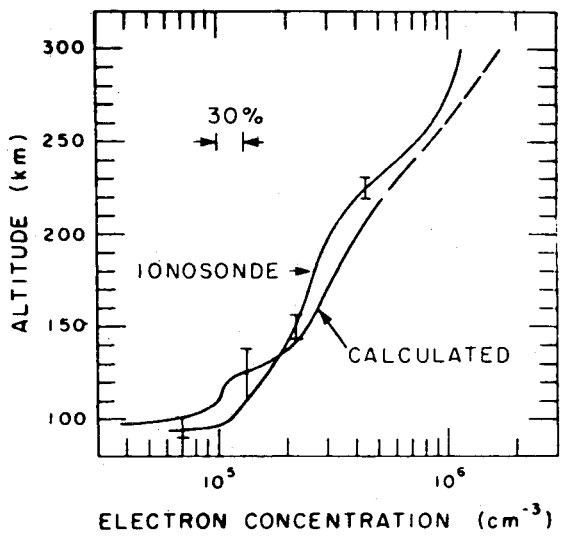

Fig. 1 Calculated and observed[27] electron concentration vs altitude. The estimated errors given for the ionosonde measurement are 0 to +30 km near 120 km and ±5 km elsewhere. Calculated concentrations above 220 km shown as dotted curve. Solar zenith angle was 27 deg.

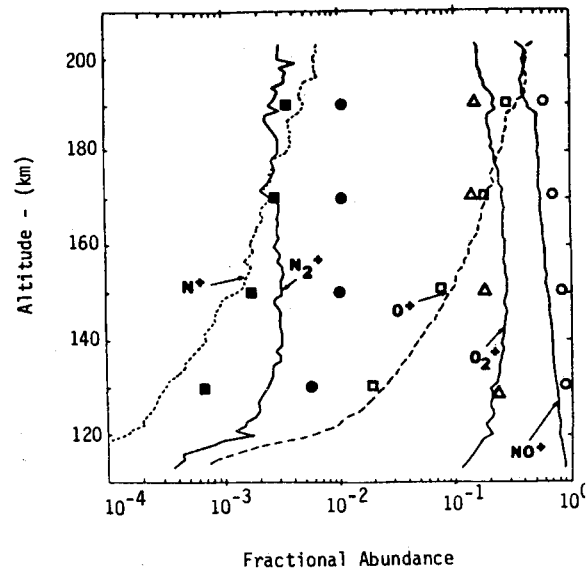

Fig. 2 Fractional ion abundances for the continuous aurora. Data are given by the solid and broken curves and come from Swider and Narcisi.[28]

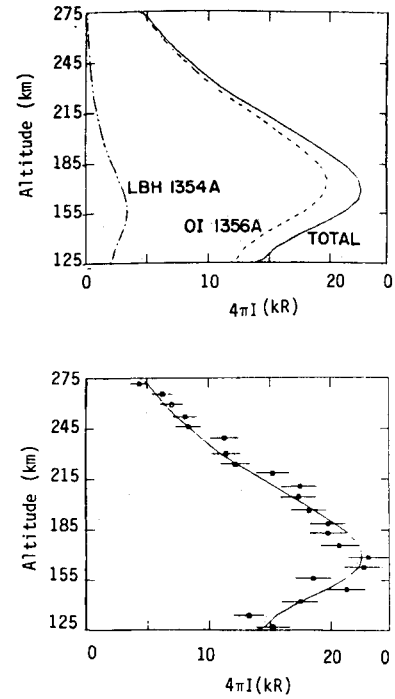

Fig. 3 1356 Å dayglow limb intensity. Data are from Newman and Christensen[17,19] while calculations are from Strickland and Anderson.[29]

Daytime Results

In this section, we wish to demonstrate the variability of optical emissions and n_e caused by changes in the solar

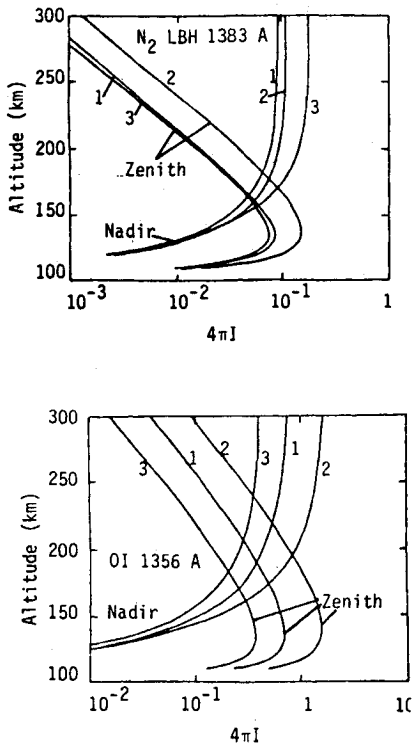

Fig. 4 Zenith and nadir viewing OI 1356 Å and N_2 LBH 1383 Å dayglow intensities. The solar zenith angle is 60 deg. The labeling refers to the following conditions: 1) low solar activity, Jacchia 1977 $n(0)$; 2) high solar activity, Jacchia 1977 $n(0)$; 3) low solar activity, half of Jacchia 1977 $n(0)$.

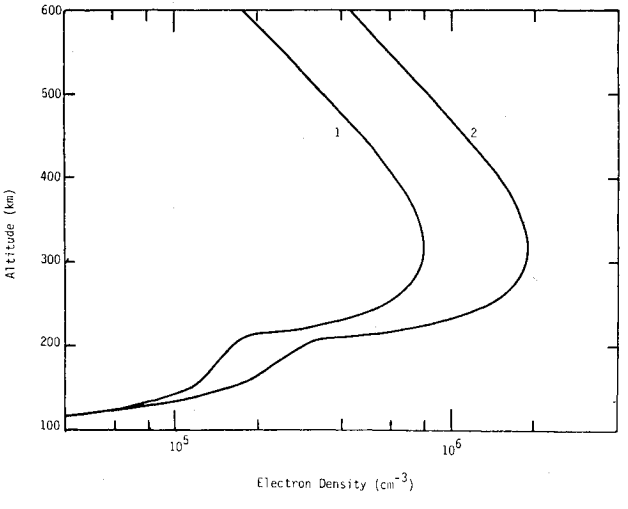

Fig. 5 Calculated daytime electron density. Labeling is the same as in Fig. 4.

activity and the neutral densities. We have just begun addressing this problem and will restrict the results to two key optical features and three starting conditions. The features to be considered are LBH 1383 Å [the (2,0) and (5,2) bands] and OI 1356 Å. Both features are at sufficiently short wavelengths that Rayleigh scattering of solar radiation does not contaminate their intensities on emerging from the ionosphere. Conditions are defined in terms of solar activity (indexed by $F_{10.7}$, the 10.7 cm solar flux) and the model atmosphere. We use solar spectrum representations from Torr et al.[31] for high ($F_{10.7} = 207$) and low ($F_{10.7} = 71$) activity. The basic model atmosphere comes from the 1977 Jacchia model.[12] One set of results will be shown for which the O density has been reduced by half.

Figure 4 shows nadir and zenith viewing intensities for the three sets of starting conditions. We observe a change in intensity of ~ 2 in going from low to high solar activity. As expected, halving the atomic oxygen density reduces the OI 1356 Å intensity by a similar factor. The LBH 1383 Å intensity is altered only slightly because of a small reapportionment of photoelectron energy received by N_2. As we mentioned above, the actual variation in OI 1356 Å due to solar variability may be less than our calculations indicate. If so, it may be that the Torr et al.[31] solar spectra overestimate the amount of euv variability. This problem remains under investigation.

Figure 5 shows electron densities for the two levels of solar activity. The results above 200 km include the effect of diffusion. We regard these results as preliminary, since they are the first we have obtained for daytime conditions and since the diffusion model is still under development. Although they are preliminary, the results for the two sets of conditions are sufficient for demonstrating the variability in the electron density profile and its relationship to corresponding variability in optical intensities.

Nighttime Auroral Results

In the previous section, we observed that changes in source conditions (changes in solar activity) lead to changes in emission brightness without noticeably affecting relative emission strengths. It is, thus, the absolute intensities of optical features that concern us in the daytime ionosphere with regard to monitoring variations in the source spectrum. The situation is noticeably different in the auroral ionosphere, where a wide range of altitude profiles can exist in volume excitation and emission rates due to variability in the hardness of the incident electron spectrum. This leads to some significant variations in relative intensities, since changes in the above altitude profiles affect excitation efficiencies and the extent to which pure absorption and quenching operate. We shall now examine such variations for the purpose of determining how well one can hope to characterize the source spectrum from optical measurements.

Intensities have been calculated for viewing in the nadir direction from above the emitting region. The incident spectrum is described by a Maxwellian distribution having the form

$$\phi_0(E,\mu) = \left(\frac{Q_M}{2\pi E_M^3}\right) E\exp(-E/E_M)\,\mathrm{e/cm^2\text{-}s\text{-}eV\text{-}sr}$$

where E and μ are, respectively, the electron energy and cosine of the pitch angle, E_M is the characteristic energy, and Q_M is the energy flux. Calculations have been performed for $Q_M = 1$ erg/cm^2-s and for E_M values over the range from 0.5 to 5 keV. Figures 6a and 6b show the calculated intensities of the features under consideration as functions of E_M. A Jacchia 1977 model atmosphere was used for all calculations. We observe varying amounts of decrease for all features except N_2^+ 3914 and LBH 1273 Å. The decreases in Fig. 6a are caused primarily by the increasing amount of O_2 pure absorption. Some of the decrease at 1356 Å is also caused by a decreasing excitation efficiency for atomic oxygen. Pure absorption has little effect at 1273 or 3914 Å, or at the wavelengths considered in Fig. 6b. The decreases exhibited at 2762 and 2972 Å are caused primarily by quenching. Some of the decrease at 2972 Å, as at 1356 Å, is also caused by a decreasing excitation efficiency. The states from which these emissions arise are $N_2(A\,^3\Sigma)$ and $O(^1S)$, which are coupled in the sense that an important source of ^1S excitation comes from the reaction

$$N_2(A) + O \rightarrow N_2(X) + O(^1S)$$

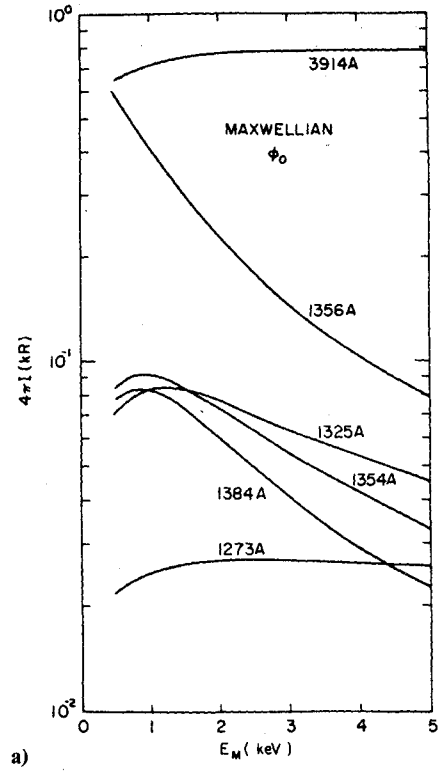

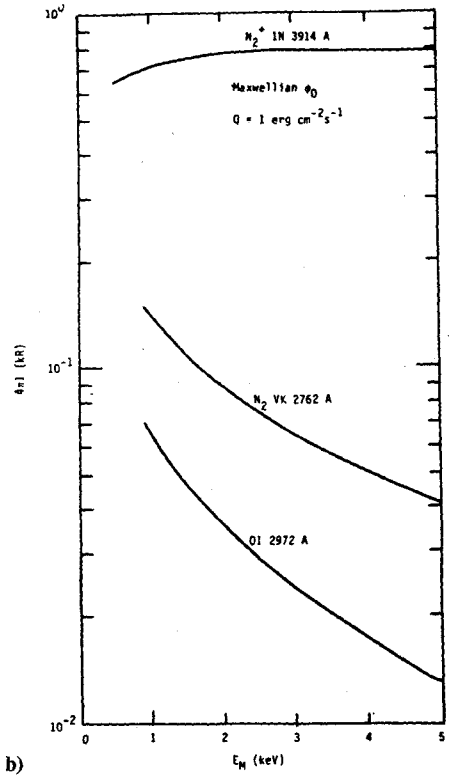

Fig. 6 Nadir viewing auroral intensities as functions of the incident electron spectrum. Spectra are represented by Maxwellian distributions where E_M is the Maxwellian characteristic energy.

The more prominent emission from the ^{1}S state is at 5577 Å, which we have excluded because its nadir-observed intensity is contaminated by emission and scattering below the ionosphere. The 3914 Å intensity will also be affected by scattering and albedo, but in spite of this we include it in Fig. 6 since it is one of the most prominent and frequently observed uv features in the aurora.

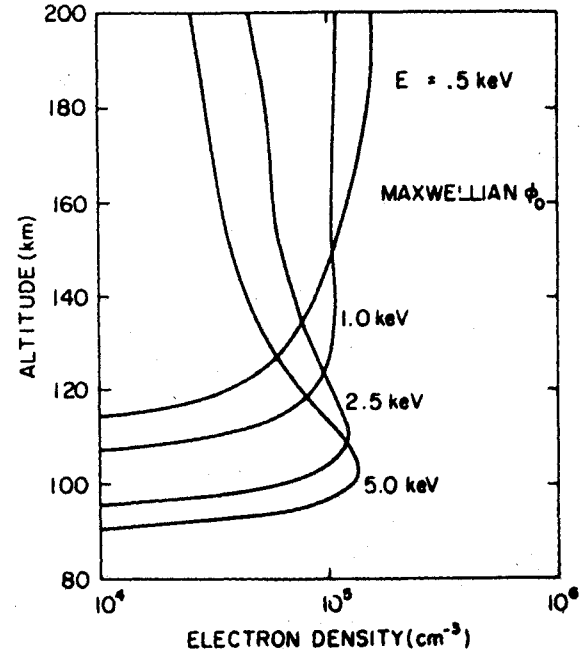

Fig. 7 Auroral E region electron densities for four different incident electron spectra represented by Maxwellian distributions.

We have obtained profiles similar to those shown in Fig. 6 for other model atmospheres. In particular, we have scaled the O_2 and O densities in various ways to generate these models. As expected, the most notable changes have come from scaling the O density. The OI 1356 Å intensity varies nearly directly with the O scaling factor because the main source is direct excitation of O(^{5}S) with a small contribution (~ 10%) from dissociative excitation of O_2. Little effect is observed in the N_2 emissions. Thus, this intensity is potentially valuable for monitoring either source conditions or the O density, depending on how well these are known from independent information. We should note that multiple scattering of the 1356 Å photons does occur, but has only a minor effect for the given viewing conditions.[29,30]

The final results we wish to consider are electron densities and, in particular, the sensitivity of their altitude profiles to changes in the source spectrum. Figure 7 illustrates this sensitivity in which we show four profiles for characteristic energies of 0.5, 1, 2.5, and 5 keV. Since most of our attention until recently has been directed to the auroral E region, we choose here to limit our discussion to the behavior of n_e under chemical equilibrium conditions. For all results, $Q_M = 1$ erg/cm^2-s as before. We do observe noticeable changes in the n_e profiles shown, although not in maximum values. It is worth comparing results such as these to results for other types of source representations. We have done so by carrying out a series of calculations for incident electron spectra characterized by narrow Gaussian distributions.[4] We find the overall profile to be similar where respective characteristic energies are chosen to give the same altitude of maximum ionization. For the more nearly monoenergetic Gaussian source, however, n_e peaks somewhat more sharply and does not penetrate as deeply into the atmosphere.

Much more can be said about the results presented in this section. We have limited the discussion, in part because details are available elsewhere,[4] and our emphasis is meant to be on the larger picture of just how much potential optical observations hold for monitoring the ionosphere. We complete this paper in the next section with some general comments at this level of consideration.

Discussion

Clearly, we have not answered the question of just how effectively n_e and the major neutral densities, especially $n(0)$,

can be monitored by optical techniques. This is a difficult question which first requires statements of the needed accuracy in the deduced quantities and of instrument capability. Given this information, we can then proceed to incorporate results of the type discussed in this paper into a statistical analysis, out of which come deduced density profiles with associated standard deviations for specific optical data sets. This should be done initially under ideal conditions, which means that these deviations would not reflect uncertainties introduced by winds and fields.

What we are able to say at this time is that selected uv features do show sufficient variability in their intensities to make it worthwhile to proceed with the kind of analysis discussed above. We shall be continuing our investigation along these lines with an important part of this work directed to those complications which remove us from ideal modeling conditions. Among such complications not previously mentioned are the nonanalytic nature of actual auroral electron spectra and incomplete spectroscopic information (see, e.g., Refs. 32 and 33).

Acknowledgments

This work was partially sponsored by the DMSP Program Office, Space Division, Air Force Systems Command.

References

[1]Chandra, S., Reed, E.I., Meier, R.R., Opal, C.B., and Hicks, G.T., "Remote Sensing of the Ionospheric F Layer by Use of OI 6300 Å and OI 1356 Å Observations," *Journal of Geophysical Research*, Vol. 80, No. 16, 1975, pp. 2327-2332.

[2]Tinsley, B.A. and Bittencourt, J.A., "Determination of the F Region Height and Peak Electron Density at Night Using Airglow Emissions from Atomic Oxygen," *Journal of Geophysical Research*, Vol. 80, No. 16, 1975, pp. 2333-2337.

[3]Feldman, P.D., Anderson, D.E., Jr., Meier, R.R., and Gentieu, E.P., "The Ultraviolet Dayglow 4. The Spectrum and Excitation of Singly Ionized Oxygen," *Journal of Geophysical Research*, Vol. 86, No. A5, 1981, pp. 3583-3588.

[4]Strickland, D.J., Jasperse, J.R., and Whalen, J.A., "Dependence of Auroral FUV Emissions on the Incident Electron Spectrum and Neutral Atmosphere," *Journal of Geophysical Research*, 1983, in press.

[5]Bauer, S.J., *Physics of Planetary Ionospheres*, Springer-Verlag, New York, 1973, pp. 185-189.

[6]Evans, J.V., "The Dynamics of the Ionosphere and Upper Atmosphere," in *Physics of Solar Planetary Environment*, American Geophysical Union, Washington D.C., 1976, pp. 630-671.

[7]Hargreaves, J.K., *The Upper Atmosphere and Solar Terrestrial Relations*, Van Nostrand Reinhold, New York, 1979, pp. 72-74.

[8]Banks, P.M. and Kockarts, G., *Aeronomy*, Academic Press, New York, 1973, pp. 169-190.

[9]Prolss, G.W., "Perturbation of the Low-Latitude Upper Atmosphere During Magnetic Substorm Activity," *Journal of Geophysical Research*, Vol. 87, No. A7, 1982, pp. 5260-5266.

[10]Ossakow, S.L., "Ionospheric Irregularities," *Reviews of Geophysics and Space Physics*, Vol. 17, No. 4, 1979, pp. 521-533.

[11]Fejer, B.G. and Kelley, M.C., "Ionospheric Irregularities," *Reviews of Geophysics and Space Physics*, Vol. 18, No. 2, 1980, pp. 401-454.

[12]Jacchia, L.G., "Thermospheric Temperature, Density, and Composition: New Models," *Spec. Rep., 375*, Smithsonian Astrophysical Observatory, Cambridge, Mass. 1977.

[13]Hedin, A.E., Salah, J.E., Evans, J.V., Reber, C.A., Newton, G.P., Spencer, N.W., Kayser, P.C., Alcayde, D., Bauer, P., Cogger, L., and McClure J.P., "A Global Thermospheric Model Based on Mass Spectrometer and Incoherent Scatter Data, MSIS 1, N_2 Density and Temperature," *Journal of Geophysical Research*, Vol. 82, No. 16, 1977, pp. 2139-2147.

[14]Hedin, A.E., Reber, C.A., Newton, G.P., Spencer, N.W., Brinton, H.C., Mayr, H.G. and Potter, W.E., "A Global Thermospheric Model Based on Mass Spectrometer and Incoherent Scatter Data, MSIS 2, Composition," *Journal of Geophysical Research*, Vol. 82, No. 16, 1977, pp. 2148-2156.

[15]Barlier, F., Berger, C., Falin, J.L., Kockarts, G., and Thuillier, G., "A Thermospheric Model Based on Satellite Drag Data," *Annals of Geophysics*, Vol. 34, 1978, pp. 9-24.

[16]Hedin, A.E., Spencer, N.W., Mayr, H.G., and Porter, H.S., "Semi-empirical Modeling of Thermospheric Magnetic Storms," *Journal of Geophysical Research*, Vol. 86, No. A5, 1981, pp. 3515-3518.

[17]Newman, A.L., Christensen, A.B., and Anderson, D.E., Jr., "Atomic Oxygen Density Deduced From Limb-Scans of the UV Dayglow," *Journal of Geophysical Research*, Vol. 88, No. A11, 1983, pp. 9265-9270.

[18]Meier, R.R. and Anderson, D.E., Jr., "Determination of Atmospheric Composition and Temperature from the UV Airglow," *Planetary and Space Sciences*, Vol. 31, 1983.

[19]Christensen, A.B., Newman, A.L., and Anderson, D.E., Jr., "Results of a Satellite-Borne Limb Scanning UV Spectrometer From Remote Sensing of Atmospheric Density," *21*st Aerospace Sciences Meeting, Reno, Nev., Jan. 1983.

[20]Meier, R.R., Strickland, D.J., Feldman, P.D., and Gentieu, E.P., "The Ultraviolet Dayglow, 1. Far UV Emissions of N and N_2," *Journal of Geophysical Research*, Vol. 85, May 1982, pp. 2177-2184.

[21]Jasperse, J.R., "Boltzmann-Fokker-Planck Model for the Electron Distribution Function in the Earth's Ionosphere," *Planetary and Space Sciences*, Vol. 24, 1976, pp. 33-40.

[22]Jasperse, J.R., "Electron Distribution Function and Ion Concentrations in the Earth's Lower Ionosphere From Boltzmann-Fokker-Planck Theory," *Planetary and Space Sciences*, Vol. 25, 1977, pp. 743-756.

[23]Strickland, D.J. and Meier, R.R., "A Photoelectron Model for the Rapid Computation of Atmospheric Excitation Rates," National Research Laboratories Memorandum Report 5004, 1982.

[24]Strickland, D.J., Book, D.L., Coffey, T.P., and Fedder, J.A., "Transport Equation Techniques for the Deposition of Auroral Electrons," *Journal of Geophysical Research*, Vol. 81, No. 16, 1976, pp. 2755-2764.

[25]Spiger, R.J., and Anderson, H.R., "Electron Currents Associated with an Auroral Band," *Journal of Geophysical Research*, Vol. 80, No. 16, 1975, pp. 2161-2164.

[26]Craven, J.D. and Frank, L.A., "Electron Angular Distributions Above the Day Side Auroral Oval," *Journal of Geophysical Research*, Vol. 81, No. 10, 1976, pp. 1695-1699.

[27]Neroux, L., Cohen, M., and Higgens, J.E., "Electron Densities Between 110 and 300 km Derived from Solar EUV Fluxes of August 23, 1972," *Journal of Geophysical Research*, Vol. 79, No. 34, 1974, pp. 5237-5244.

[28]Swider, W. and Narcisi, R.J., "Problems with the $N_2^+ + O \rightarrow NO^+ + N$ Reaction in Aurora," *Geophysical Research Letters*, Vol. 8, No. 12, 1981, pp. 1239-1241.

[29]Strickland, D.J. and Anderson, D.E., Jr., "Radiation Transport Effects on the 1356 Å Limit Intensity Profile in the Dayglow," *Journal of Geophysical Research*, Vol. 88, No. A11, 1983, pp. 9260-9264.

[30]Anderson, D.E., Jr., Meier, R.R., Feldman, P.D., and Gentieu, E.P., The UV Dayglow 3. OI Emissions at 989, 1027, 1304, and 1356 Å," *Geophysical Research Letters*, Vol. 7, No. 12, 1980, pp. 1057-1060.

[31]Torr, M.R., Torr, D.G., Ong, R.A., and Hinteregger, H.E., "Ionization Frequencies for Major Thermospheric Constituents as a Function of Solar Cycle 21," *Geophysical Research Letters*, Vol. 6, No. 10, 1979, pp. 711-744.

[32]Huffman, R.E., LeBlanc, F.J., Larrabee, J.C., and Paulson, D.E., "Satellite Vacuum Ultraviolet Airglow and Auroral Observations," *Journal of Geophysical Research*, Vol. 85, No. A5, 1980, pp. 2201-2215.

[33]McLaughlin, R.W., Erdman, P.W., and Zipf, E.C., "On the Excitation of the N_2 LBH System in the Airglow and Aurora," *EOS, Transactions, American Geophysical Union*, Vol. 63, No. 18, 1982, p. 394.